

Laser annealing protocols for healing radiation-damaged single-photon detectors

Joanna Krynski, Nigar Sultana, Youn Seok-Lee, Jin Gyu Lim, Vadim Makarov, Thomas Jennewein

Abstract—Radiation-induced dark count rate in previously irradiated silicon avalanche photo diodes is significantly reduced in a thermal vacuum environment through annealing of the detector active area with a high-power laser using varying annealing protocols.

Keywords—avalanche photodiode, single-photon detectors, laser annealing, quantum communications, displacement damage

Corresponding (and Presenting) Author:

J. Krynski, Department of Physics and Astronomy and Institute for Quantum Computing, University of Waterloo, Waterloo, ON, Canada.

Contributing Authors:

N. Sultana, Department of Physics and Astronomy and Institute for Quantum Computing, University of Waterloo, Waterloo, ON, Canada.

Y. Seok-Leo, Department of Physics and Astronomy and Institute for Quantum Computing, University of Waterloo, Waterloo, ON, Canada

Jin Gyu Lim, Department of Physics and Astronomy and Institute for Quantum Computing, University of Waterloo, Waterloo, ON, Canada

Vadim Makarov, Department of Physics and Astronomy and Institute for Quantum Computing, University of Waterloo, Waterloo, ON, Canada

Thomas Jennewein, Department of Physics and Astronomy and Institute for Quantum Computing, University of Waterloo, Waterloo, ON, Canada

Presentation Preference: Poster Presentation

Session Preference:

ACKNOWLEDGEMENTS

This research is funded by through the Canadian Space Agency FAST Grant, as well as through the Canadian Foundation for Innovation.

I. INTRODUCTION

SINGLE-PHOTON avalanche photodiodes (SPADs) are used in various fields, including for applications in remote sensing and LIDAR [1], medical imaging [2], [3] and classical communications [4]. SPADs have also been extensively used in space, where their ease of integration and operation, as well as wide spectral sensitivity out-compete other single-photon detectors such as photomultiplier tubes and superconducting nanowires [5]. SPADs will be particularly integral in the facilitation of a global quantum communication network as their high detection efficiency, low timing jitter, low dark count rate and low afterpulsing probability make them prime candidates for inter-node satellite quantum receivers [6], [7]. There has already been demonstration of long-distance satellite-based quantum communication by the Micius satellite and many more missions are to be launched in the near future [8], [9], [10].

One dominant issue each mission must consider is the impact of space radiation on SPADs' dark count rates (DCR), as it is well-known that radiation degrades detector performance, particularly dark count rate [11],[12],[13]. This issue is critical for quantum communication purposes where a dark count rate of below 200 cps is required to facilitate a high-fidelity transmission of information [7]. Previous terrestrial and in-orbit studies have used thermal annealing as method of controlling the radiation-induced increase in DCR [14], [15], [8]. Another method that has been shown to be successful in reducing dark counts is optical annealing via a high-power (on the order of 1W) laser [16], [17]. This method provides an advantage in that it delivers highly localized uniform heating straight to the active area when the beam is fiber-coupled to the detector package. In-orbit annealing of SPADs actively being damaged by space radiation will soon be observed via the Cool Annealing Payload satellite (CAPSat) which was deployed from the ISS on October 12, 2021 [18], [19].

The protocols for laser annealing are still not well-established and must be designed such that the limited communication time with the space craft is maximized to take useful measurements. The present study tests three protocols for annealing radiation-damaged SPADs by varying the laser power and annealing timing. We anneal four fiber-coupled SPADs with very high initial dark count rates (>300 kcps) and significant saturation effects with annealing powers of over 2 W and for annealing durations of up to 16 minutes. We report up to 48 times reduction of DCR as well as evidence of improvement in SPAD sensitivity and alleviation of saturation.

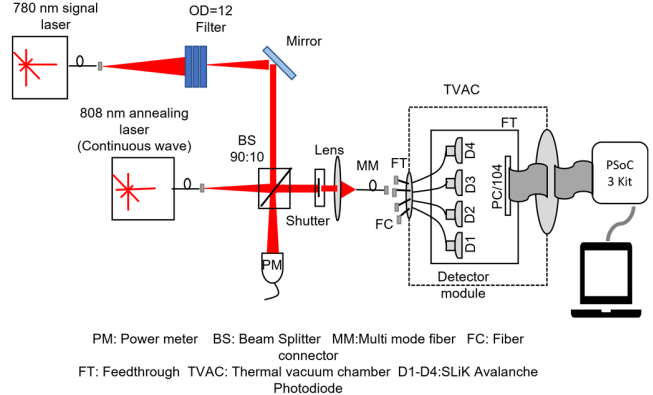


Fig. 1. Schematic of optical set-up.

II. EXPERIMENTAL SET-UP

The four samples to be annealed are silicon single-photon APDs (Excelitas SLiK, 180 μ m active area), custom-built with fiber connectors intended to focus the beam onto the active area. The SPADs were previously irradiated by 105 MeV protons, to a fluence equivalent to 10.5-years in low-Earth orbit (2×10^{10} protons/cm 2) and then repeatedly thermally annealed [15]. The four samples are mounted to an aluminum and the bracket is attached to the detector module (DM) PCB. The DM PCB possesses circuitry to bias, quench and readout the SPADs individually, as well control SPAD active area temperature via their internal thermoelectric cooler (TEC). Control of the DM is conducted via the externally connected Cypress PSOC3 development kit.

Figure 1 shows a schematic of the set-up, which is comprised of bench-top optics and the PSOC3 kit at room pressure, and the DM inside a thermal vacuum chamber (TVAC) at an average pressure of 10^{-6} torr (~0.001 atm). On the optics side, a high power multimode 808 nm laser diode is used for annealing, while a tunable 780 nm laser diode is used to test SPAD sensitivity (signal laser). The annealing laser beam is collimated by a lens, then is incident on a 90:10 beamsplitter. 10% of the beam is measured by a power meter and 90% of the beam reflects towards a fast electric-shutter where it is focused by a lens into a multimode (MM) fiber which terminates at one of the SPADs in the TVAC. The signal laser is also coupled to this MM fiber eventually, after being attenuated to single-photon level using several neutral density filters. The DM electrical wires are covered in vacuum-suitable jackets and are connected to the PSOC via another feedthrough. The PSOC3 controls the DM and facilitates read out in a terminal program (*TeraTerm*) via a serial connection to the PSOC. The data collected included those related to DM operational status (such as TEC current) as well as those related to SPADs (such as dark count rate).

III. METHODS

A. Laser annealing protocols

Three laser annealing protocols were tested: (a) Variable annealing power with fixed 3 min exposure time; (b) Variable duration, single exposure time and fixed annealing power; and (c) Variable duration, repeated exposure time and fixed annealing power. The difference between schemes (b) and (c) is that the former anneals the SPAD active area with a certain duration once, while the latter anneals the SPAD with a certain duration three times. SPAD characterization occurs after each annealing exposure. Table 1 summarizes the range of annealing powers and duration of exposures.

TABLE I
ANNEALING PROTOCOLS

Protocol	SPAD	Annealing Power (W)	Maximum Annealing Time (mins)
Variable Power	1	0 – 2.3	3
Variable Time	2	1.5	14
	3	1.2	16
	4	1.8	16

The annealing power described in the table is the power measured at the end of the MM fiber which connects to the SPAD package. For each round of annealing, the annealing power is set by increasing the bias current of the 808 nm laser until the power meter reads the correct value (based on a previously constructed calibration curve). The fast shutter is opened for a pre-determined exposure duration, allowing the SPAD active area to be annealed. The SPADs are not biased during annealing, therefore, the temperature of the active area is not known during the annealing exposure. However, resistance temperature detectors are placed on the DM in various places, giving an insight into the heating process of the area surrounding the annealed detector. Once the exposure time is reached, the fast shutter is closed and the annealing laser is turned off. The detectors are left unbiased for another several minutes to ensure that any local heating in the active area is cooled down.

B. Characterization

Characterization is conducted with the lab in complete darkness to block out as much background light as possible. Measurements are taken at three TEC set temperatures: -22° C, -10°C and 0°C. After approximately 60s of temperature stabilization, the SPAD is biased to 6V above breakdown. This voltage is unusually low for these

SLiK-type SPAD, which typically operate at 20V above breakdown when undamaged. However, it was found prior to annealing that these particular samples have such high dark counts that they exhibit saturation effects at about 12V above breakdown. Therefore, detection efficiency is sacrificed for being below the saturation point [20]. For each temperature, dark counts from the selected SPAD are logged once per second for 1 minute while the laser annealing beam is off and while the fast-shutter is closed. In a similar fashion, for each temperature, counts from the selected SPAD are logged while the fast-shutter is open and the 780 nm signal laser is exposed to the SPAD active area. A measurement of detector counts with respect to excess bias is also conducted as a method of observing any changes in the SPAD saturation point. Additional characterization of the SPADs, such as jitter or recharge time, is not possible due to inaccessibility of the DM within the TVAC.

IV. RESULTS

A. Variable annealing power

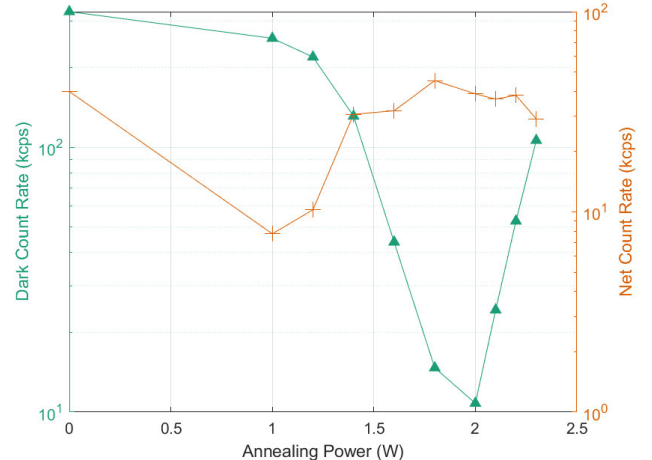


Fig. 2. (a) SPAD 1 dark count rate and net count rate as a function of annealing laser power, measured after 3 minutes exposure to annealing beam.

Annealing with a power of less than 1W for a fixed 3-minute exposure with variable annealing power does not yield significant decrease in dark count rate. DCR decreases noticeably after exposure to 1W beam and continues to decrease until 2W exposure. The pre-annealing DCR was 325 kilocounts per second (kcps) and the lowest DCR achieved after annealing is 10.8 kcps, resulting in a dark count reduction factor (DCRF) of about 30 for a SPAD operation temperature of -22°C. All annealing exposure greater than 2W result in an increase in DCR, likely indicating that damage is being done to the SPAD active area.

Count rates with the signal laser turned on are very similar to when the signal laser is turned off (dark count rate) before annealing. After 1W annealing, a divergence begins between the count rate with signal laser on versus off. The signal count rate follows the trend of the DCR with respect to the decrease in count rate until 2W annealing and then a rise in count rate afterward, however, the signal count rate does not drop as dramatically as the dark count rate. This is emphasized in Figure 1, where the net count rate (right y-axis), or the difference between signal and dark count rates, is plotted.

B. Variable annealing time

The other three SPAD samples are annealed separately at one of 1.2, 1.5 and 1.8 W, as this range of annealing powers yields a noticeable reduction in DCR and increase in SPAD 1 sensitivity.

Larger annealing power yields a steeper decrease in DCR with the most drastic decrease in DCR after the first short exposures. Longer exposure time does not appear to reduce DCR more than short exposure times. A plateau in the DCR is seen in all three cases of a fixed annealing power with very long exposure times. The DCRF for 1.2 W, 1.5 W and 1.8 W annealing tests is 2, 12 and 48, respectively. In the interest of confirming that this plateau is indeed the lowest achievable DCR for each annealing power, the SPADs are annealed with 1.8 W or more for 3 minutes. In the case of the SPAD 1 and SPAD 2 annealed with 1.2 W and 1.5 W, respectively, an additional burst of 2 W annealing further reduced the DCR significantly, while for the SPAD annealed at 1.8 W, the DCR actually rose after the 2 W exposure. Although on the whole the DCR decreased in the SPAD annealed at 1.8 W, the final spike in DCR after the higher annealing power burst, as well as the staggered descent of the DCR to the plateau level, indicates that an annealing power greater than 1.8 W is damaging the SPAD active area.

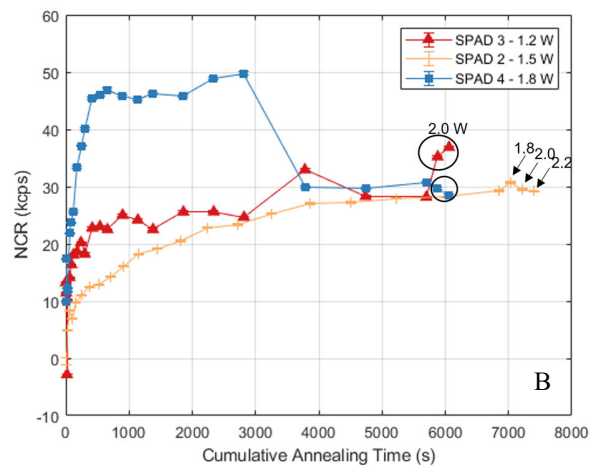
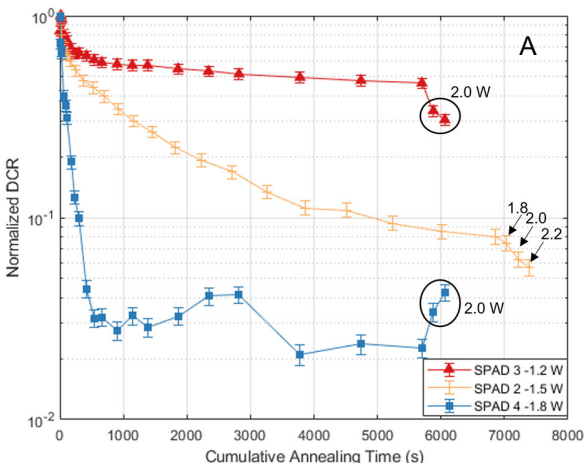


Fig. 3. SPAD 2, 3, 4 (a) normalized dark count rate and (b) net count rate as a function of cumulative annealing time, measured after 3 minutes exposure to annealing beam. Annotated points indicate exposures with higher annealing power.

The NCR of each SPAD after annealing (Figure 3b) exhibits a trend of tending towards a count rate of around 30 kcps, despite an interesting discrepancy between the two lower annealing powers and the highest annealing power. The sharp drop in NCR of the 1.8 W annealed SPAD after 3000s of cumulative annealing time coincides with a drop in a steep decrease in signal count rate. While this is not the largest decrease in either signal or dark count rate that is observed throughout the measurements, it does mark a difference in the magnitude of decrease between the signal and dark count rates, which tend to change at the same rate before and after this one anomalous measurement. Since nothing changed in the characterization process or in the surrounding environment, this deviation is likely due to some reorganization of the defects in the semiconductor lattice such that the photoexcited carriers are more suppressed than the thermally excited carriers. After the last two rounds of 1.8 W annealing, both signal and dark count rates decrease similarly and NCR continues to tend towards 30 kcps, which indicates that annealing rearranged spurred permanent changes in the semiconductor.

C. Repeated annealing exposure

In both exposure schemes (single and triple) the change in dark count rate is largest for the earliest annealing rounds and then diminishes with later annealing exposures. However, the triple-exposed SPADs' DCRs exhibit higher fluctuations notably after every third exposure when the annealing time is extended. The

greatest reductions in DCR occur after the first exposure at 10, 60, 180 and 480 s, and the reductions after the two subsequent exposures of the same duration are much smaller. The larger fluctuations cannot be attributed to a higher annealing power, since the effect is seen in the lowest annealed SPAD (1.2 W) as well as the highest annealed

SPAD (1.8 W).

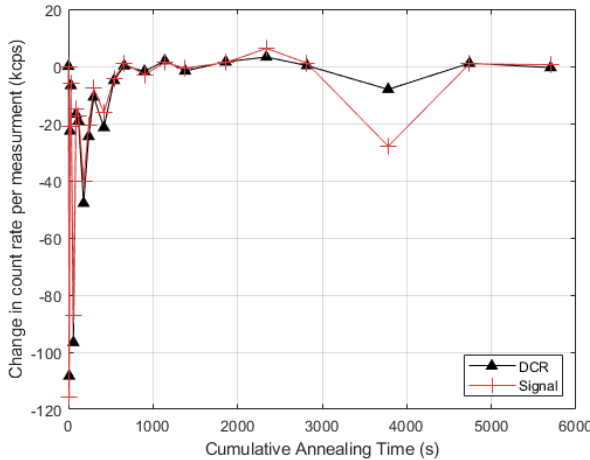


Fig. 4. SPAD 4 change in dark and signal count rate between annealing rounds (at 1.8 W).

D. Reduction of detector saturation

Saturation in SPADs is defined by a decrease in count rate despite an increase in bias voltage. Prior to annealing we find the saturation point to be about 12 V above breakdown. We find that saturation appears to decrease with every annealing round, as evidenced by the saturation point occurring at a higher bias voltage in subsequent measurement as compared to previous measurements. .

V. CONCLUSION

We show in this study that laser annealing can be a potent method of reducing dark counts in noisy detectors such that previously indistinguishable signal counts can be clearly resolved from background noise. It appears that annealing power is a more critical parameter than laser annealing time: much greater reduction of dark count rates was achieved with higher powers. We suggest that annealing also increases sensitivity of the detector at a fixed bias due to the diminishing of saturation effects. Our results agree with [16] in that little change is seen for powers less than 1W. Annealing at such high powers has not yet been demonstrated before in a fiber-coupled system and shows that even long exposures of the SPAD active area can tolerate very high intensity stimulation. This result may come with the caveat that the SPADs must suffer from a very high dark count rate, such as those seen after an extended period in space or after a

particularly large radiation event such as after a solar flare. Repeated high power annealing can be reserved for cases of highly damaged detectors, while smaller bursts can be regularly applied to manage daily accumulation of dark count rate.

REFERENCES

- [1] M. A. Krainak, W. Y. Anthony, G. Yang, S. X. Li, and X. Sun, ‘Photon-counting detectors for space-based laser receivers’, in *Quantum Sensing and Nanophotonic Devices VII*, 2010, vol. 7608, p. 760827.
- [2] D. Palubiak, M. M. El-Desouki, O. Marinov, M. J. Deen, and Q. Fang, ‘High-Speed, Single-Photon Avalanche-Photodiode Imager for Biomedical Applications’, *IEEE Sensors Journal*, vol. 11, no. 10, pp. 2401–2412, 2011,
- [3] Y. Mu and M. Niedre, ‘Fast single photon avalanche photodiode-based time-resolved diffuse optical tomography scanner’, *Biomed. Opt. Express*, vol. 6, no. 9, pp. 3596–3609, Sep. 2015
- [4] B. Steindl, M. Hofbauer, K. Schneider-Hornstein, P. Brandl, and H. Zimmermann, ‘Single-photon avalanche photodiode based fiber optic receiver for up to 200 Mb/s’, *IEEE Journal of Selected Topics in Quantum Electronics*, vol. 24, no. 2, pp. 1–8, 2017.
- [5] R. H. Hadfield, ‘Single-photon detectors for optical quantum information applications’, *Nature photonics*, vol. 3, no. 12, pp. 696–705, 2009.
- [6] Y.-S. Kim, Y.-C. Jeong, S. Sauge, V. Makarov, and Y.-H. Kim, ‘Ultralow noise single-photon detector based on Si avalanche photodiode’, *Review of scientific instruments*, vol. 82, no. 9, p. 093110, 2011.
- [7] J.-P. Bourgoin *et al.*, ‘A comprehensive design and performance analysis of LEO satellite quantum communication’, *arXiv preprint arXiv:1211.2733*, 2012.
- [8] M. Yang *et al.*, ‘Spaceborne, low-noise, single-photon detection for satellite-based quantum communications’, *Optics express*, vol. 27, no. 25, pp. 36114–36128, 2019.
- [9] T. Jennewein *et al.*, ‘QEYSSAT: a mission proposal for a quantum receiver in space’, in *Advances in photonics of quantum computing, memory, and communication VII*, 2014, vol. 8997, p. 89970A.
- [10] R. Bedington, J. M. Arrazola, and A. Ling, ‘Progress in satellite quantum key distribution’, *npj Quantum Information*, vol. 3, no. 1, pp. 1–13, 2017.
- [11] X. Sun, D. Reusser, H. Dautet, and J. B. Abshire, ‘Measurement of proton radiation damage to Si avalanche photodiodes’, *IEEE transactions on Electron Devices*, vol. 44, no. 12, pp. 2160–2166, 1997.
- [12] Y. C. Tan, R. Chandrasekara, C. Cheng, and A. Ling, ‘Silicon avalanche photodiode operation and lifetime analysis for small satellites’, *Optics express*, vol. 21, no. 14, pp. 16946–16954, 2013.
- [13] F. Moscatelli *et al.*, ‘Radiation tests of single photon avalanche diode for space applications’, *Nuclear Instruments and Methods in Physics Research Section A: Accelerators, Spectrometers, Detectors and Associated Equipment*, vol. 711, pp. 65–72, 2013.
- [14] E. Anisimova *et al.*, ‘Mitigating radiation damage of single photon detectors for space applications’, *EPJ Quantum Technology*, vol. 4, pp. 1–14, 2017.
- [15] I. DSouza *et al.*, ‘Repeated radiation damage and thermal annealing of avalanche photodiodes’, *EPJ Quantum Technology*, vol. 8, no. 1, p. 13, 2021.
- [16] J. G. Lim, E. Anisimova, B. L. Higgins, J.-P. Bourgoin, T. Jennewein, and V. Makarov, ‘Laser annealing heals radiation damage in avalanche photodiodes’, *EPJ quantum technology*, vol. 4, pp. 1–16, 2017.
- [17] A. N. Bugge, S. Sauge, A. M. M. Ghazali, J. Skaar, L. Lydersen, and V. Makarov, ‘Laser damage helps the eavesdropper in quantum cryptography’, *Physical review letters*, vol. 112, no. 7, p. 070503, 2014.
- [18] S. Schwink, ‘Self-annealing photon detector brings global quantum internet one step closer to feasibility’. [Online]. Available: <https://physics.illinois.edu/news/CAPSat-in-orbit>
- [19] N. Sultana, ‘Single-photon detectors for satellite based quantum communications’, PhD Thesis, University of Waterloo, 2020.
- [20] S. Cova, M. Ghioni, A. Lacaita, C. Samori, and F. Zappa, ‘Avalanche photodiodes and quenching circuits for single-photon detection’, *Applied optics*, vol. 35, no. 12, pp. 1956–1976, 1996.